Water Solubilized Indigo

DOI: 10.1002/anie.201203236

Laponite Blue: Dissolving the Insoluble**

*Marina M. Lezhnina, Tobias Grewe, Hardo Stoehr, and Ulrich Kynast**

Solubility issues are among the most frequently encountered problems for chemical experimentalists. This holds true for the laboratory scale, but often poses a bottleneck in industrial exploitation as well. Solubility problems arise from two possible directions: dissolution of nonpolar entities into polar media, or vice versa. Herein we present the dissolution of the nonpolar dye indigo, which is not normally encountered in aqueous solution. Its utterly surprising mobilization into the aqueous phase is facilitated with relative ease by the aid of nanoscopic clay shuttles, which consecutively form a nanoclay hybrid, in strong reminiscence of the famous Maya Blue pigment.

Generally, clay minerals are an extraordinarily versatile class of materials, with technical uses ranging from ordinary pottery to high-tech medical applications.[1] Maya Blue is a historic, cultural, and aesthetic facet, which has fascinated numerous chemists and archaeologists alike.[2] Its chemical nature was only unraveled in the 1960s:[3] it is an ancient example for a hybrid material, more specifically, an inorganic–organic hybrid.[4]

On the inorganic side, Maya Blue is based on the clay mineral palygorskite, a layered silicate of an idealized composition $(Mg,Al)_5[(Si,Al)_8O_{20}](OH)_2(OH_2)_4{\cdot}4H_2O$.[5] The organic constituent of the hybrid, indigo (Figure 1a), has been known for 4000 years, and it is still the most heavily exploited organic blue dye.[6] Intra- and intermolecular hydrogen bonds account for the poor solubility of pure, crystalline indigo.[7] Inserted into palygorskite layer interspaces, the visible absorption of indigo provides the optical function to make Maya Blue a colorant with a blue to turquoise tint. Owing to its insolubility in both ordinary organic and inorganic solvents, the Maya Blue indigo–palygorskite hybrid must be classified as a pigment, which thus had to be applied as a dispersion or slurry. Apart from past and ongoing research on Maya Blue itself, recent efforts have been devoted to the accommodation in other microporous structures, such as silicalite[8] and other zeolitic hosts.[9] Furthermore, dyes other than indigo have been inserted into palygorskites, thereby expanding the color range and thus affording a range of novel hybrid pigments.[10]

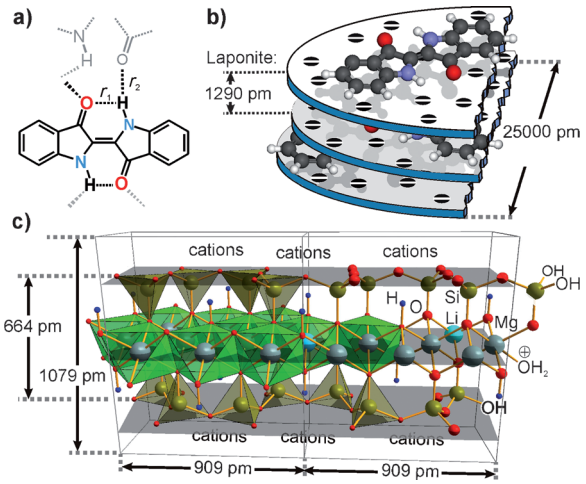

Figure 1. Components of the Laponite Blue hybrid. a) Molecular structure of indigo. Intramolecular ($r_1 = 226$ pm) and intermolecular hydrogen bonds ($r_2 = 211$ pm) as found in pure indigo[7] are indicated as dots. b) Solid laponite: cations (or other guest molecules, not to scale) link individual, negatively charged platelets, eventually to form stacks of laponite. c) Structure of laponite: side view of two unit cells, (100) direction. The dimensions refer to a single crystal structure analysis of Cs-hectorite,[11] from which the depicted slab has been reconstructed.

Morphologically related to palygorskite is the natural clay mineral hectorite;[11] nanoscaled synthetic derivatives of these, namely laponites, are available commercially.[12] Much to our delight, the marriage between indigo and Laponite RD afforded a water-soluble hybrid, which we term Laponite Blue, as its aqueous solutions closely mimic solid Maya Blue and indigo optically. Laponite RD, the host material of concern here (chemical composition $Na_{0.7}[Mg_{5.5}Li_{0.3}Si_8O_{20}(OH)_4](H_2O)_n$), consists of layers of $[SiO_4]$ tetrahedra sandwiching sheets of Mg^{2+}, which complement their octahedral coordination by bridging OH groups (Figure 1c). The microstructure of Laponite RD is best described as strongly anisotropic platelets that are characterized by a primary particle diameter of approximately 25 nm and a thickness of the platelets of less than 1 nm. Partial substitution of Mg^{2+} in the octahedral sheets by Li^+ charges the faces of the platelets negatively, such that cations (Na^+ natively, in addition to as much as 15% of water) are accommodated on or between the faces of the platelets (interlayers) for charge compensation in the solid powders (Figure 1b).

As indicated in Figure 1c, the rims of the platelets bear dangling oxygen atoms (Si–OH and Mg–OH), which, depending on pH, may be protonated or ionized. In con-

[*] Dr. M. M. Lezhnina,[+] T. Grewe, Dr. H. Stoehr, Prof. Dr. U. Kynast
Institute for Optical Technologies
Münster University of Applied Sciences
Stegerwaldstrasse 39, 48565 Steinfurt (Germany)
E-mail: uk@fh-muenster.de
[+] Presently on leave from Mari Technical State University Yoshkar-Ola, Institute of Physics
Lenin-pl. 3, 424000 Yoshkar-Ola (Russia)

[**] M.M.L. and U.K. are greatly indebted to BASF Coatings GmbH, Münster (Germany), for financial support.
Supporting information for this article is available on the WWW under http://dx.doi.org/10.1002/anie.201203236.

junction with the very small sizes, the assembly of ionizable species at the faces and rims of the platelets yields a ready solubility of the nanoclays in aqueous solution at concentrations below 5 wt%, although there are more complex interpretations beyond this simplified description.[13]

On dispersing the laponite in water, Na^+ cations leave the interlayers, and at the same time delaminate the stacked platelets to individual disks. The mobile Na^+ cations may also be ion-exchanged by a broad variety of other cations, such as cationic dyes and luminophores.[14] However, the laponite surprisingly proved to also be capable of adsorbing neutral organic molecules and allowed their eventual transportation into aqueous solution, as demonstrated here for the notoriously insoluble indigo. This behavior is of different origin than the effect termed "adsolubilization", which utilizes surfactants,[15] but may to some degree be reminiscent of the adsorption of perylene on a solid laponite clay.[16]

The uptake of indigo by laponite was investigated from both chloroform solution and by the gas phase. A heterogeneous uptake of indigo from $CHCl_3$ is also possible, but proved to be less suitable, because it led to colloidal crystals adhering to the laponite surface, which after filtration and redispersion in water segregated floccules of indigo after a few days. In contrast, gas-phase loading, which started with mixtures of the powderous materials, led to superior reproducibility, homogeneity of solid samples, and stability of the eventual dispersions. For the materials presented in the following, solid indigo and laponite were thoroughly ground in a mortar and heated stepwise in vacuum up to 150 °C, on which the laponite loses approximately three occluded water molecules (thermogravimetrical analysis; Supporting Information, Figure S4). Owing to the large surface of the nanoscaled clay ($>221\ m^2 g^{-1}$) and corresponding reactivity or adsorption susceptibility, color variations and inhomogeneities, as reported for indigo loaded micrometer-sized palygorskite powders,[17,18] were not observed. Instead, a fairly wide series of water-soluble Laponite Blue could be prepared (Figure 2a).

Finally, the absorption spectra presented in Figure 3 were monitored for laponite loadings of 50 to 450 molecules of indigo per individual laponite platelet with respect to the idealized, anhydrous composition; the quantifying term molecules per platelet (MpP) seems to be an appropriate concentration designator in this context. Taking an area of roughly 1.3 nm^2 for an indigo molecule, these loadings would correspond to an approximate surface coverage from 3–30% of fully delaminated laponite, or an average distance between indigo molecules ranging from 4.4–1.5 nm. It should be emphasized that the 0.25 wt% solutions were visually clear for the whole concentration range after simple centrifugation, which on first sight appears to contradict the absorption spectra. It appears incongruous that the initial indigo concentration and absorbance do not correlate linearly. This behavior finds its explanation in the slow formation of colloidal indigo aggregates at higher loads that adhere to the clay carrier initially. Visible aggregates only appear as the coverage of the clay platelets exceeds approximately 150 dye molecules per disk and can readily be identified by X-ray diffraction peaks of indigo in the composite powders. As

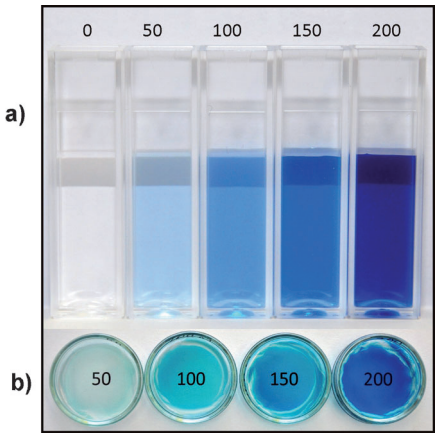

Figure 2. Photographic images of Laponite Blue solutions and films. The numbers given represent amounts of indigo molecules actually used per platelet (MpP) in the preparation, calculated on the basis of anhydrous laponite (analytical, true amounts are approximately 50% lower, ranging from 22 to 109 MpP; see the Supporting Information, Tables S1 and S2). a) Aqueous solutions with a constant amount of laponite (0.25 wt%) but increasing concentrations of indigo (50–200 MpP); higher amounts of laponite concentrations of up to 3 wt% are possible, but lead to increasing viscosities. b) Transparent Laponite Blue layers (approximately 7 μm thick) after solvent evaporation. Color changes are discussed in the text.

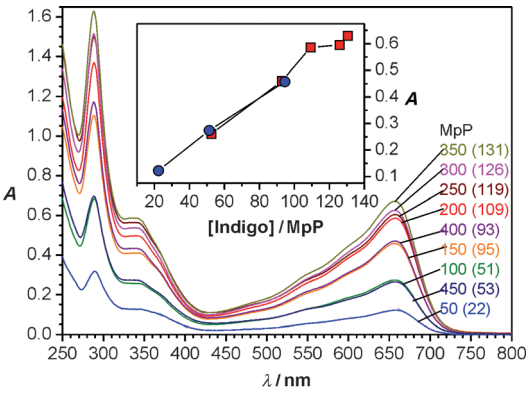

Figure 3. UV/Vis absorbance of hybrids with varying indigo content, expressed as MpP. The MpP values refer to the initial amounts of indigo used for preparation of the powders; data in brackets refer to analytically determined true amounts after work-up. Although the redispersion to 0.25 wt% solutions appears visually to be complete after stirring for two hours (see Figure 2a), for the spectroscopic characterization, the take-up period was extended to 15 h to ensure equilibration. The spectra were thus obtained after dilution to 0.0625 wt% of laponite for adjustment of the absorbance to a value below 1 at 657 nm (1 cm cuvettes). Further, for complete removal of scattering agglomerates, the solutions were centrifuged at 17000 rpm (20 min) and filtered through a 0.2 μm PVDF membrane prior to the absorption measurements. Inset: Absorbance at 657 nm replotted after chemical analysis of laponite and indigo dispersions and recalculation of the "true" contents. Blue circles: initial load ≤150 MpP; red squares: initial load >150 MpP. (See also the Supporting Information, Table S2 for true concentrations).

opposed to that, powders with initially ≤150 MpP show no sign of crystalline indigo after heating (Supporting Information, Figure S2). However, consecutive work-up, that is, centrifugation and filtration procedures, lead to the removal

of some indigo for low contents samples as well and, to a much lesser degree (< 10 %), of laponite agglomerates (Supporting Information, Experimental Section, Tables S1, S2). The work-up thus remedied undesired scatter and established almost complete linearity. Inevitably, the procedures obviously go at the cost of overall indigo concentration (that is, lowering of the MpP by roughly 50 %), as apparent from Figure 3 (inset) and the Supporting Information, Table S2.

In line with the agglomeration of indigo as concluded from X-ray data, an IR absorption at 1392 cm^{-1} appears as the initial dye load exceeds about 150 MpP. As in crystalline indigo, this vibration is assigned to an −N−H deformation (δ) that involves intermolecular hydrogen bonding (N−H···O=C)[19,20] and also found in indigo–sepiolite hybrids.[21] Significantly opposed to that, a vibration at 1412 cm^{-1}, attributed to δ N−H···O=C with intramolecular interaction, is retained even on adsorption to the laponite (Supporting Information, Figure S3), while the vanishing intermolecular 1392 cm^{-1} band yields information on the state of indigo association and can therefore serve as added proof for the (predominant) presence of monomolecular indigo on the laponite at lower loading levels.[20] This extensive review on sepiolite based Maya Blue also hints that the interaction of indigo with laponite might be weaker than in Maya Blue, as band splittings of, for example, the 1462 cm^{-1} band (ν(C−C) and d(C−H) are absent.

Consequently, but not at all surprisingly, Laponite Blue with adsorbed or intercalated guests, that is, in solution or the solid state, respectively, does not exhibit the stability of hybrids, where the indigo is occluded in channels of the host structures.[22] Laponite, being a swellable clay, thus exposing the indigo directly to chemical action, cannot be expected to compete with Maya Blue, but still experiences an appreciable stabilization in standard tests[3a] as in conc. HCl, and against extraction with actone and chloroform (Supporting Information, Table S3).

Furthermore, X-ray diffraction of powders recovered by evaporation of the water solvent additionally reveals that the indigo is aligned parallel to the faces of the platelets, at least in the solid, as evident from the lattice constant in *c*-direction (perpendicular to layers), which amounts to 1.29 nm as compared to 1.28 nm of pure laponite (Supporting Information, Figure S2). Whether or not intercalated or adhering water supports the hydrogen bonding modes cannot be decided conclusively from the vibrational spectra, but the somewhat reduced width and intensity of the H−O−H deformation modes and an emerging structure in comparison to free laponite favor the involvement of interlayered water (Supporting Information, Figure S3c). Furthermore, the adsorption of indigo also strongly reduces the amount of loosely bonded intercalated water by approximately 40 H_2O/indigo in the solid materials; however, an appreciable amount of tightly bound water persists, as can be derived from differential thermogravimetry (DTG) data (Supporting Information, Figure S4 and Table S2). The spectral behavior of thin films, briefly described in the last paragraph, also supports this assumption.

Returning to the absorption spectra, the visible π→π* transition found at 657 nm is strongly red-shifted in comparison to solutions in benzene (595 nm[23]), $CHCl_3$, (602 nm,[24a] 604 nm[24b]), DMF (610 nm[24a]), or DMSO (620 nm[25,26]), which is readily interpreted in terms of the merocyanine effect, that is, a bathochromic shift of the absorption with polarity. The extinction coefficient ε for the transition was found to be constant at 10300 $L\,mol^{-1}\,cm^{-1}$ in the concentration range between 0.047×10^{-3} and 0.177×10^{-3} $mol\,L^{-1}$ and eventual loadings of 22–95 MpP (pure indigo in DMF: $\varepsilon_{max}=22\times140$ $L\,mol^{-1}\,cm^{-1}$ at 610 nm[27]). An absorption wavelength as high as 657 nm has not previously been observed for indigo in solution, but resembles that of the solid-state reflectance spectra reported for synthetic Maya Blue[17,18,26] (Supporting Information, Figure S5).

Finally, the spectral behavior of thin films of Laponite Blue (Figure 2b; Supporting Information, Figure S5) indicates that adhering or intercalated water may participate in bonding, as the visible absorption reversibly blue-shifts to 637 nm on drying (loss of water, that is, polarity), while rewetting re-establishes the 657 nm band. Within the environments discussed, the laponite as such evidently provides the highest polarity, which is enhanced even further owing to co-adherence of water. However, while the proposition of a synergistic involvement of hydrogen bonds to the laponite seems reasonable for indigo adsorption, further investigative efforts will have to be devoted to the detailed mechanisms underlying the adherence of species void of OH and NH groups, for example, aromatics like the beforementioned perylenes.[16] Evidence for changes in the absorption spectra as reported for the latter and ascribed to the formation of a radical cation, is not observed for indigo. Indigoid derivatives (dehydroindigo[23,26] and leucoindigo[26–29]) have been reported to accompany both historical and synthetic Maya Blue,[28] and may also be identified on inspection of other synthetic sources[17,18,26] by an absorption band at 442 nm. The photophysics of dehydroindigo in solvents and attapulgite matrix has recently been described theoretically and further confirmed experimentally.[26] However, although very small amounts of dehydroindigo seem to appear in the FTIR spectra (Supporting Information, Figure S3c) of Laponite Blue as well,[20,28,29] corresponding absorptions are practically lacking in the laponite hybrid in solution, films, and powder samples.

We have found other examples for unexpected aqueous solubilization, such as the normally insoluble, efficiently luminescing rare-earth diketonate complex $[Eu(tta)_3(phen)]$ (tta = tris[1-(2-thenyl)-4,4,4-trifluorbutane-1,3-dionate], phen = 1,10-phenanthroline),[30] and Lumogen F Red 305, which belongs to a class of perylene dyes that have been the subject of extensive research into solar-cell concentrators.[31]

In summary, by exploiting the highly charged surface of nanoclays, the nonpolar dye indigo can be solubilized into aqueous solution. A novel hybrid material is obtained, which strongly resembles the ancient Maya Blue pigment optically. Although predominantly devoted to spectral analogies of the Maya Blue pigment here, the underlying solubilization concept may replenish the chemistry of colorants and coatings more generally; evidently, this can embrace neutral lumines-

cent dyes for photonic applications, such as bioassays or safety marking. Last but not least, beyond optical functionalization, the operationality of nonpolar, neutral species in waterborne photo- and homogeneous catalysis may be augmented by soluble nanoclays as well, and will be a subject of future investigations.

Received: April 27, 2012
Published online: September 5, 2012

Keywords: absorption · adsorption · clays · dyes/pigments · organic–inorganic hybrid composites

[1] F. Bergay, B. K. G. Theng, G. Lagaly in *Handbook of Clay Science*, *Vol. 1*, Elsevier, Amsterdam, **2006**.
[2] a) M. S. del Rio, A. Domenech, M. T. Domenech-Carbo, M. L. V. de Agredos Pascual, M. Suarez, E. Garcia-Romero in *Developments in Palygorskite-Sepiolite Research*, *Vol. 3* (Eds.: E. Galàn, A. Singer), Elsevier, Amsterdam, **2011**, pp. 453 – 482; b) A. Doménech, M. T. Doménech-Carbo, M. L. V. de Agredos Pascual, *Angew. Chem.* **2011**, *123*, 5859; *Angew. Chem. Int. Ed.* **2011**, *50*, 5741.
[3] a) R. J. Gettens, *Am. Antiq.* **1962**, *27*, 557; b) A. O. Shepard, *Am. Antiq.* **1962**, *27*, 565; c) H. van Olphen, *Science* **1966**, *154*, 645.
[4] a) P. Gómez-Romero, C. Sanchez, *New J. Chem.* **2005**, *29*, 57; b) G. Chiari, R. Giustetto, G. Ricchiardi, *Eur. J. Mineral.* **2003**, *15*, 21.
[5] P. Gómez-Romero, C. Sanchez in *Functional Hybrid Materials* (Eds.: P. Gómez-Romero, C. Sanchez), Wiley-VCH, Weinheim, **2005**, pp. 1 – 14.
[6] E. Steingruber in *Ullmann's Encyclopedia of Industrial Chemistry*, Wiley-VCH, Weinheim, **2004**, DOI: 10.1002/14356007.a14_149.pub2.
[7] a) H. von Eller, *Bull. Soc. Chim. Fr.* **1955**, *106*, 1433; b) P. Süsse, M. Steins, V. Kupcik, *Z. Kristallogr.* **1988**, *184*, 269.
[8] C. Dejoie, P. Martinetto, E. Dooryhee, P. Strobel, S. Blanc, P. Bordat, R. Brown, F. Porcher, M. S. del Rio, M. Anne, *ACS Appl. Mater. Interfaces* **2010**, *2*, 2308.
[9] a) C. Dejoie, P. Martinetto, E. Dooryhee, E. van Elsalande, S. Blanc, P. Bordat, R. Brown, F. Porcher, M. Anne, *Appl. Spectrosc.* **2010**, *64*, 1131; b) S. Kowalak, A. Zywert, *Clay Miner.* **2011**, *46*, 197.
[10] a) R. Giustetto, K. Seenivasan, D. Pellerej, G. Ricchiardi, S. Bordiga, *Microporous Mesoporous Mater.* **2012**, *155*, 167; b) R. Giustetto, O. Wahyudi, *Microporous Mesoporous Mater.* **2011**, *142*, 221.
[11] J. Breu, W. Seidl, A. Stoll, *Z. Anorg. Allg. Chem.* **2003**, *629*, 503.
[12] Rockwood Additives, http://www.rockwoodadditives.com/laponite/brochure.asp, **2010**.
[13] a) G. Lagaly, S. Ziesmer, *Adv. Colloid Interface Sci.* **2003**, *100 – 102*, 105; b) A. Mourchid, A. Delville, J. Lambard, E. Lecolier, P. Levitz, *Langmuir* **1995**, *11*, 1942; c) P. Levitz, E. Lecolier, A. Mourchid, A. Delville, S. Lyonnard, *Europhys. Lett.* **2000**, *49*, 672; d) B. Ruzicka, L. Zulian, G. Ruocco, *Langmuir* **2006**, *22*, 1106.
[14] a) J. Bujdák, *Appl. Clay Sci.* **2006**, *34*, 58; b) R. Sasai, T. Itoh, W. Ohmori, H. Itoh, M. Kusunoki, *J. Phys. Chem. C* **2009**, *113*, 415; c) M. V. Martínez, F. L. Arbeloa, J. P. Prieto, I. L. Arbeloa, *J. Phys. Chem. B* **2005**, *109*, 7443; d) J. Cenens, R. A. Schoonheydt, *Clays Clay Miner.* **1988**, *36*, 214; e) R. A. Schoonheydt, L. Heughebaert, *Clay Miner.* **1992**, *27*, 91; f) S. A. Hussain, R. A. Schoonheydt, *Langmuir* **2010**, *26*, 11870; g) T. Nakamura, J. K. Thomas, *Langmuir* **1985**, *1*, 568; h) J. K. Thomas, *Acc. Chem. Res.* **1988**, *21*, 275.
[15] a) K. Esumi, Y. Takeda, M. Goino, K. Ishiduki, F. Koide, *Langmuir* **1997**, *13*, 2585; b) K. Esumi, Y. Takeda, Y. Koide, *Colloids Surf. A* **1998**, *135*, 59.
[16] a) X. Liu, J. K. Thomas, *Langmuir* **1991**, *7*, 2808; b) X. X. Liu, K. K. Iu, J. K. Thomas, *Langmuir* **1992**, *8*, 539.
[17] D. Reinen, P. Köhl, C. Müller, *Z. Anorg. Allg. Chem.* **2004**, *630*, 97.
[18] a) A. Doménech, M. T. Doménech-Carbo, M. S. del Rio, S. Goberna, E. Lima, *J. Phys. Chem. C* **2009**, *113*, 12118; b) A. Doménech, M. T. Doménech-Carbo, M. S. del Rio, M. L. V. de Agredos Pascual, E. Limad, *New J. Chem.* **2009**, *33*, 2371.
[19] a) E. Tatsch, B. Schradert, *J. Raman Spectrosc.* **1995**, *26*, 467; b) A. Baran, A. Fiedler, H. Schulz, M. Baranska, *Anal. Methods* **2010**, *2*, 1372.
[20] R. Giustetto, K. Seenivasan, F. Bonino, G. Ricchardi, S. Bordiga, M. R. Chierotti, R. Gobetto, *J. Phys. Chem. C* **2011**, *115*, 16764.
[21] S. Ovarlez, F. Giulieri, A. M. Chaze, F. Delamare, J. Raya, J. Hirschinger, *Chem. Eur. J.* **2009**, *15*, 11326.
[22] a) R. Giustetto, O. Wahyudi, I. Corazzari, F. Turci, *Appl. Clay Sci.* **2011**, *52*, 41; b) M. Sanchez del Rio, P. Martinetto, C. Reyes-Valerio, E. Doorhyee, M. Suarez, *Archaeometry* **2006**, *48*, 115.
[23] D. Jacquemin, J. Preat, V. Wathelet, A. Perpète, *J. Chem. Phys.* **2006**, *124*, 074104 – 1.
[24] a) M. M. Sousa, C. Miguel, I. Rodrigues, A. J. Parola, F. Pina, J. S. Seixas de Melo, M. J. Melo, *Photochem. Photobiol. Sci.* **2008**, *7*, 1353; b) G. Weinstein, J. M. Wyman, *J. Am. Chem. Soc.* **1956**, *78*, 2387.
[25] G. Haucke, G. Graness, *Angew. Chem.* **1995**, *107*, 116; *Angew. Chem. Int. Ed. Engl.* **1995**, *34*, 67.
[26] a) J. Seixas de Melo, R. Rondao, H. D. Burrows, M. J. Melo, S. Navaratnam, R. Edge, G. Voss, *J. Phys. Chem. A* **2006**, *110*, 13653; b) R. Rondão, J. S. Seixas de Melo, V. D. B. Bonifacio, M. J. Melo, *J. Phys. Chem. A* **2010**, *114*, 1699.
[27] J. Seixas de Melo, A. P. Moura, M. J. Melo, *J. Phys. Chem. A* **2004**, *108*, 6975.
[28] A. Doménech, M. T. Doménech-Carbo, M. L. Vazquez de Agredos Pascual, *J. Phys. Chem. B* **2006**, *110*, 6027.
[29] M. Klessinger, W. Lüttke, *Tetrahedron* **1963**, *19 (Suppl. 2)*, 315.
[30] P. Klauth, M. Rietz, J. Bueddefeld, U. Kynast, M. Lezhnina, DE 102009024673A1, **2010**, WO 002010115503A3, **2011**.
[31] a) J. C. Goldschmidt, M. Peters, A. Bösch, H. Helmers, F. Dimroth, S. W. Glunz, G. Willeke, *Sol. Energy Mater. Sol. Cells* **2009**, *93*, 176; b) M. G. Debije, P. P. C. Verbunt, *Adv. Energy Mater.* **2012**, *2*, 12.

